Geoderma 338 (2019) 430–444

Contents lists available at ScienceDirect

Geoderma

journal homepage: www.elsevier.com/locate/geoderma

Laser diffraction analysis of aggregate stability and disintegration in forest and grassland soils of northern Minnesota, USA

Chase S. Kasmerchak[a,*], Joseph A. Mason[b], Mengyu Liang[b]

[a] Department of Geography, Environment, and Spatial Sciences, 673 Auditorium RD, Michigan State University, East Lansing, MI 48823, United States
[b] Department of Geography, 550 North Park Street, University of Wisconsin, Madison, WI 53706, United States

ARTICLE INFO

Handling Editor: M. Vepraskas

Keywords:
Aggregate stability
Laser diffraction
Soil chemistry
Soil organic matter
Forest-grassland ecotone

ABSTRACT

A method for characterizing aggregate stability with repeated laser diffraction measurements was tested on soils spanning the prairie-forest ecotone in northern Minnesota, USA. These soils formed in similar parent material but display a wide range of upper horizon morphology, organic carbon content, and chemistry, allowing assessment of the method's performance over a wide range of aggregate stability and its utility in identifying factors influencing aggregate behavior. Equations representing fine material release through breakdown of two aggregate populations as first-order processes were fit to experimental data. The best-fit parameters for these equations, and an additional index of persistent water-stable aggregate content, indicated distinct differences in aggregate behavior among the major horizons of Mollisols and Alfisols. Linear models were developed to explore the relationships between these parameters and soil physicochemical characteristics for the dataset as a whole and for subsets corresponding to four zones with different vegetation history, soil orders, and major soil horizons. The relationships identified were relatively weak (R^2 = 0.30 to 0.70). The best predictors for the parameters representing early disintegration of less stable aggregates were cation exchange capacity (CEC) and effective CEC (ECEC) for the whole dataset, although organic carbon and nitrogen contents also emerged as predictors for forest and Alfisol subsets. The best predictors for the index of persistent water-stable aggregate content were organic carbon content, base saturation, or exchangeable Ca/Mg ratio, depending on the particular subset and fine material size fraction used in the analysis. The relatively weak explanatory power of organic carbon content as a predictor of aggregate behavior in these experiments was somewhat surprising, given prior work on aggregate stability. Both CEC and ECEC may serve as proxies for the various combinations of organic matter and clay content that influence aggregate stability in these samples, explaining their importance as predictors. It is likely that other factors not examined in this research contributed to aggregate stability, including carbonate content, clay mineralogy, and differing frequency and types of pedoturbation under grassland and forest. The results of this study are relevant to reconstructing the development of texture-contrast profiles as forest invaded grassland over the past 4000 in the study area, as documented by paleoecological research. In particular, loss of organic matter below a thin A horizon may have facilitated initial development of an E horizon in which weak aggregation favored clay eluviation; loss of clay would then have weakened aggregate stability still further. We suggest this new method for assessing aggregate stability can also be applied to research on soil erosion and runoff potential as affected by land use and management.

1. Introduction

The processes of infiltration under rainfall, soil crust formation, soil erosion and sedimentation are all influenced by the stability and disintegration of aggregates as water interacts with soil (Le Bissonnais, 1996; Green and Hairsine, 2004; Singer and Shainberg, 2004). In addition, research on the role of aggregation in the accumulation and turnover of OM has a long history (Six et al., 2004) and has recently assumed even greater importance because of its relevance to the global carbon cycle. Soil organic carbon (OC) contained within aggregates has a relatively long turnover time because of inaccessibility to microbes and/or stabilization through complexation with mineral surfaces and dissolved metal ions (Tisdall and Oades, 1982; Jastrow et al., 1996; Six et al., 1998; von Lutzow et al., 2008).

The processes that can influence aggregate stability have been recognized for many years (Six et al., 2004). These include the activities of soil fauna and microorganisms, processes associated with plant roots, physical processes such as wetting and drying or freeze-thaw cycles,

* Corresponding author.
E-mail address: kasmerch@msu.edu (C.S. Kasmerchak).

https://doi.org/10.1016/j.geoderma.2018.06.020
Received 27 November 2017; Received in revised form 12 June 2018; Accepted 17 June 2018
Available online 06 July 2018
0016-7061/ © 2018 Elsevier B.V. All rights reserved.

cultivation and other agricultural practices, and formation of inorganic cements. Especially at the scale of microaggregates (those < 250 μm), aggregation is closely linked to the addition and decomposition of organic matter (OM) and the surface chemistry of clay minerals. In particular, microaggregates develop through formation of clay-polyvalent metal cation-organic matter (C-P-OM) complexes; C-P-C and OM-P-OM complexes can also play a role (Edwards and Bremner, 1967). Tisdall and Oades (1982) introduced the concept of a hierarchy of aggregate classes differentiated by size as well as binding mechanism. Individual mineral grains and aggregates < 20 μm are bound together in 20–250 μm microaggregates, primarily by C-P-OM complex formation, and macroaggregates > 250 μm made up of smaller aggregates bound by fungal hyphae, roots, etc.

Aggregate stability is not a simple property, because it represents resistance to aggregate breakdown through several distinct processes, categorized by Le Bissonnais (1996) as slaking, physicochemical dispersion, differential swelling, and mechanical stress. Tisdall and Oades (1982) described soil behavior in which macroaggregates rapidly broke down through slaking while microaggregates resisted slaking but could be disrupted by ultrasound. Le Bissonnais and colleagues (Leguédois and Le Bissonais, 2004; Legout et al., 2005) characterized the differing stability and breakdown products of aggregates in two soils subjected to experimental slaking, mechanical stress (stirring), and rainfall impact.

Aggregate stability research is typically focused on short-term effects of soil management; however, longer-term pedogenesis can strongly influence the stability of aggregates under natural vegetation and their response to human land use change. A particularly good example is provided by the soils typically developed in subhumid mid-latitude grasslands, with deep accumulation of OM and abundant exchangeable Ca^{2+} (Neilsen and Hole, 1964; Pennock et al., 2011), both favoring aggregate stability. These properties persist to some extent even under long-term cultivation, likely making the response of these grassland soils to human land use different from that of forest soils with shallow subsurface E horizons containing much lower OM and exchangeable Ca^{2+}. From another perspective, development of highly stable or weak aggregation in upper soil horizons could potentially influence ongoing pedogenesis, particularly the key process of clay translocation. In a grassland soil with deep OM accumulation, clay particle mobilization and illuviation could be limited by stable aggregation, whereas these processes could be much more active under forest with low OM content below a thin A horizon.

Because of the importance of studying aggregate stability and disintegration over a wide range of environments and timescales, and the complexity of the processes involved, a wide variety of methods for characterizing aggregate stability and breakdown have been proposed (Amézketa, 1999; Almajmaie et al., 2017). The most well-established methods involve wet-sieving, measuring the size distribution of stable aggregates that do not break down completely, or alternatively, the fraction of stable aggregates that are retained on one size sieve, after wetting and agitation for a specific time (Nimmo and Perkins, 2002; Clement and Williams, 1958; Kemper and Rosenau, 1986; Yoder, 1936). These methods are limited in their ability to analyze size distributions of aggregates smaller than standard sieve sizes or to assess intermediate stages of disintegration.

The issue of disintegration dynamics has been addressed by methods involving progressive disruption of aggregates with ultrasound, along with repeated particle size analysis, using techniques such as the pipette/sieve method. The observed changes in apparent particle size distribution (PSD) are then characterized as a function of total disruptive energy applied (Field et al., 2006; Field and Minasny, 1999; Hunter and Busacca, 1989; Levy et al., 1993; North, 1976; Raine and So, 1993). Field and Minasny (1999) showed that aggregate disintegration can be modeled as a first-order reaction (i.e., the rate of disintegration at a given point in time is equal to a constant times the content of aggregates remaining at that point).

In the past 20 years, numerous studies have characterized aggregate breakdown using laser diffraction particle size analysis, often using repeated measurements to detect change over time or after specific treatments. Buurman et al. (1997) and Muggler et al. (1997) used laser diffraction analysis to examine aggregation in Oxisols in Brazil, comparing samples with varying degrees of dispersion. Fristensky and Grismer (2008) used laser diffraction analysis to identify subgroups of micro- and macroaggregates and to characterize their response to varying amounts of energy applied with ultrasound. Rawlins et al. (2013, 2015) described methods of aggregate stability assessment using laser diffraction measurements of the particle size distributions of aggregated soil, before and after dispersion. Two other studies observed changes in particle size distribution over time as a sample circulated in water. Westerhof et al. (1999) focused on effects of land use change on aggregates and their progressive disintegration, using repeated laser diffraction particle size distribution measurements taken at < 1, 10, 20, and 30 min of circulation. Bieganowski et al. (2010) described a method involving repeated laser diffraction measurements of a sample circulating in water at a constant rate for 30 min, which reveal progressive aggregate breakdown. Jozefaciuk and Czachor (2014) employed a similar analysis.

Mason et al. (2011) described a method in for assessing aggregate stability and disintegration similar to that of Bieganowski et al. (2010), but with longer-term measurements and a different approach to analyzing the results. The samples used by Mason et al. (2011) were sedimentary aggregates that formed from particles transported by wind from sources such as dry lake beds, rather than having formed in place in soils. Samples were suspended in deionized (DI) water, with mechanical stress applied by stirring and circulation through a particle size analyzer at a constant rate for 3 h, with no treatment by ultrasound or chemical dispersants until the end of the procedure. At that point, samples were sonicated for 3 min after addition of Na-metaphosphate (Na-MP), to produce a final, fully dispersed measurement, allowing detection of especially stable aggregates remaining after 3 h of circulation in DI water.

The method of Mason et al. (2011) allows for rapidly repeated measurements to monitor the breakdown of the least stable aggregates, which occurs within the first 10–20 min of circulation. However, it also provides information on slower but still significant ongoing breakdown that may extend over the full 3 h of analysis. The mechanical energy applied is difficult to quantify, but Mason et al. (2011) assumed that it is proportional to time of circulation and adapted the approach of Field and Minasny (1999), using circulation time as a proxy for applied energy in the following equations used to model aggregate breakdown:

$$\% > 50\ \mu m = A_0 e^{(-k_1 t)} + C_1 \quad (1)$$

$$\% < 20\ \mu m = A_0(1 - e^{(-k_2 t)}) + C_2 \quad (2)$$

where k_1 and k_2 are rate constants, t is circulation time in minutes, A_0 is the percentage of < 20 μm particles released via aggregate breakdown in the final PSD after 180 min, C_1 is the percentage of > 50 μm particles in the final PSD, and C_2 is the percentage of < 20 μm particles at $t = 0$ (minimal in some but not all cases). These equations fit most observed data quite well, although the fit was poor for a few samples.

This paper demonstrates that a modified version of the method of Mason et al. (2011) provides detailed insight on the stability and disintegration dynamics of pedogenic aggregates (formed in place in soil profiles), reveals significant contrasts between aggregates in soils affected by different natural vegetation history, and helps identify relationships between aggregate behavior and soil properties, such as OM content and cation exchange capacity (CEC). The soils are mostly under natural vegetation and aggregation within their horizons can be attributed mainly to natural, long-term pedogenic processes rather than recent soil management. We suggest, however, that the results are also relevant to understanding short-term response of these soils to changes in land cover and land use.

The aggregate stability analyses reported here were part of a larger

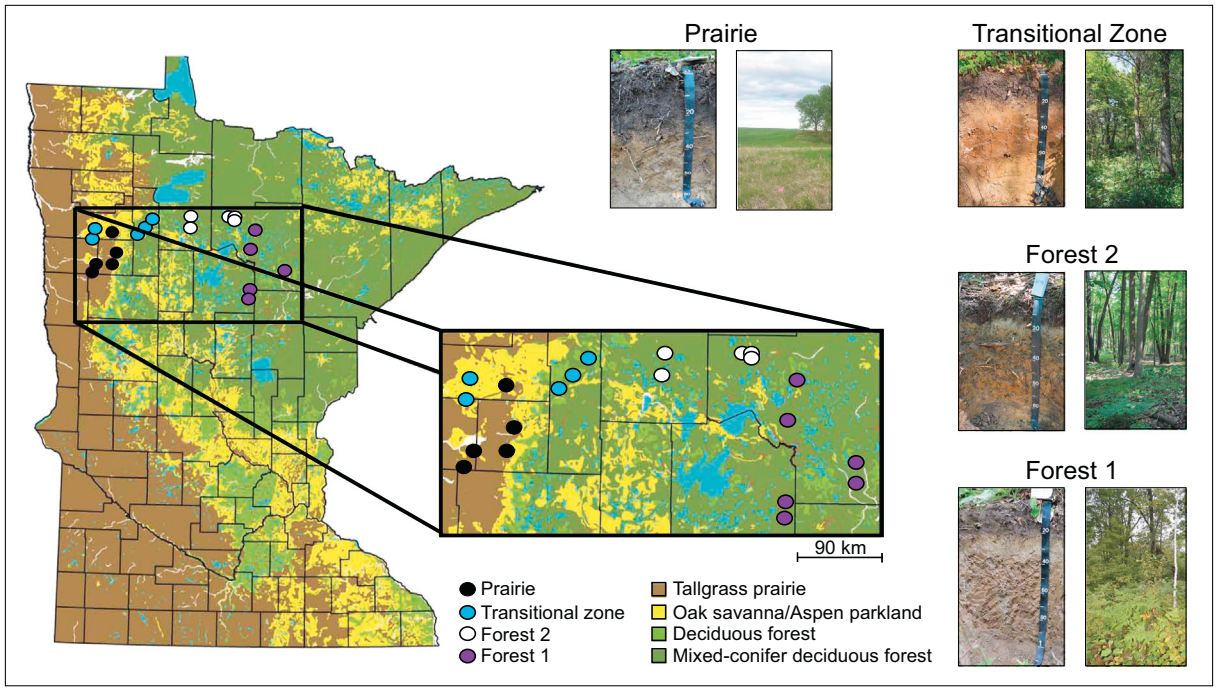

Fig. 1. Study area in northern Minnesota, USA. Examples of aboveground vegetation and soil profiles are shown for the 4 vegetation history zones examined in this research: Prairie (vegetation: site P-67; profile: site P-98), Transitional Zone (vegetation and profile: site W-70), Forest 2 (vegetation and profile: site W-44), and Forest 1 (vegetation and profile: site E-133).

study of soil response to natural vegetation change in northern Minnesota (Fig. 1), where the approximately north-south oriented boundary between forest and prairie (natural grassland) shifted substantially over the past several thousand years. A large volume of paleoecological research in this region has shown that prairie vegetation expanded eastward in the early Holocene, then retreated westward in the last 4000 yr, driven primarily by climatic change (Bartlein et al., 1984; Bradbury et al., 1993; Brugam et al., 1988; Clark et al., 2001; McAndrews, 1966, 1967; Nelson and Hu, 2008; Nelson and Hu, 2008; Jacobson and Grimm, 1986; Webb III et al., 1983; Whitlock et al., 1993; Wright, 1976).

Major contrasts in soil morphology are observed across the northern Minnesota prairie to forest transition, as it was defined by 19th century land surveys (Almendinger, 1990; Buell and Cantlon, 1951; Severson and Arneman, 1973). Soils across this ecotone formed in similar loamy glacial tills. The forest soils are Alfisols marked by A and E horizons with low clay content over clay-enriched Bt horizons. Forest A horizons are relatively thin and have weak to moderate granular structure, while E horizons have weak to very weak blocky or platy structure. The prairie soils are Mollisols with relatively uniform clay content throughout the profile and thick OM-rich A horizons with moderate to strong granular structure that persists even when exposed directly to rainfall (e.g. in rodent mounds). Soils with intermediate morphology and structural characteristics are confined to a relatively narrow transition zone. There is not a clear trend of changing morphology eastward from that transition zone, even though soils in the farthest east part of the study area have been occupied by forest for much longer – evidence that suggests a fairly rapid direct response to vegetation change rather than other factors such as climate.

The large contrasts in field-observed structural strength between prairie and forest soils led us to investigate the stability and disintegration rates of aggregates in these soils, applying methods similar to those of Mason et al. (2011). Our first objective was to test whether this method could be used to characterize and quantify contrasts in aggregate stability and the rate of aggregation disintegration in these soils, particularly those associated with the strongly differing upper horizon morphology developed under forest and prairie. Secondly, we sought to identify any significant relationships between soil physico-chemical properties (OM content, clay content, base saturation, etc.) and variables representing aggregate stability and disintegration rates, as identified by this method. These relationships were analyzed for the sample set as a whole and for groups of soils stratified by their current morphology (Alfisols vs. Mollisols) and alternatively, by their longer-term vegetation history.

2. Methods

2.1. Study area

This research was conducted on soils in northern Minnesota that span the prairie-forest ecotone as defined by 19th century public land surveys. All of the soils formed in glacial till or similarly loamy calcareous sediment of the Des Moines ice sheet lobe or its offshoot the St. Louis sublobe, deposited during the last glaciation, so soil parent material and age are held relatively constant. Modern mean annual rainfall ranges from ~735 mm yr^{-1} to ~575 mm yr^{-1} (decreasing westward) and mean annual temperature ranges from 4.70 °C to 5.69 °C (increasing westward) (National Oceanic and Atmospheric Administration 1981–2010 climate normals).

2.2. Site selection and field sampling

Samples used for aggregate analysis were from A, E (if present) and uppermost B horizons of 20 soils. These were distributed evenly across four geographic zones defined by vegetation history: prairie (P), transition zone (T), forest that replaced prairie after 4000 yr ago (F2), and forest that persisted through the Holocene (F1).

The soils were sampled within areas defined by targeted soil mapping units on slopes < 3.5°. The targeted mapping units were the predominant well-drained (or moderately well-drained in one case) upland soils in each zone that are described as having formed from glacial till. Targeted units of zones F1 and F2 were dominated by the Warba

(Haplic Glossudalfs) or Nebish (Typic Hapludalfs) series, while those in zone T were dominated by the Waukon (Mollic Hapludalfs), Chapett (Alfic Argiudolls), or Naytahwaush (Oxyaquic Hapludalfs with relatively thick, dark A horizons). Sites in zone P were in mapping units dominated by Barnes or Heimdal (both Calcic Hapludolls). All of the zone F1, F2, and T soils were under forest at the time of sampling and have not been cultivated, though most have probably been logged within the past 50–100 yr. Four of the zone P soils were under perennial non-native grass cover at the time of sampling, and all could have been cultivated for several decades, though not within the 20 years before sampling in 2013–2015, based on landowner information and/or historical aerial photography. One zone P soil was under aspen (*Populus tremuloides*) forest that probably replaced prairie within the past few hundred years.

The specific sampling sites were selected from much larger sets of randomly generated points within the targeted mapping units, based on accessibility, landowner/manager permission, and lack of recent disturbance. At each site, the upper soil profile was sampled at 25 random points and a sampling pit was located at the point where soil morphological properties (e.g. A horizon thickness, depth to Bt or Bk) were closest to the site median. The pit was excavated into the C horizon, described in detail, and sampled by subhorizon. Four of the zone P sites were sampled using three replicate hydraulic soil probe cores (7.6 cm dia.) per site rather than excavating a soil pit. Samples integrate material from the full thickness of horizons and two or three walls of the soil pit.

2.3. Analysis of aggregate behavior and stability

While larger blocky peds were disturbed in sampling, the samples used for aggregate analysis were not subsequently crushed or sieved. Two test samples were analyzed in field-moist and air-dried condition. The results (discussed below) indicated that moisture content does substantially affect some, though not all, aspects of aggregate behavior during analysis; therefore, all samples were subsequently air-dried to allow comparison at similar moisture contents. Because of the time-consuming nature of the aggregate analysis, we did not replicate it for most samples. However, three separate air-dry subsamples of two A horizons, from an Alfisol and a Mollisol, were analyzed to evaluate reproducibility (these six replicate experiments are not included in statistical analyses discussed below).

The results reported here were obtained with a Malvern Mastersizer 2000 MU laser particle size analyzer (though with only minor modification, the same procedure could be used on most laser diffraction particle sizers); all results are reported as % by volume. A beaker of 500 mL of DI water was placed in the sample module of instrument, allowing the water to circulate through the measurement cell while the water in the beaker was continuously stirred. Dry sample material was then added until the measured obscuration reached a minimum value of 2%. Repeated measurements of the apparent PSD were then taken immediately. Each measurement took about 2 min and was immediately followed by another measurement for the first 20 min of circulation; measurements were then made at approximately 10-min intervals, until the circulation time exceeded 180 min. The pump speed remained constant at 2000 rpm throughout this time; thus, aggregates in the circulating sample were subjected to a relative constant level of mechanical stress from the stirring propeller, the pump, and the effects of circulation under pressure. After 180 min, the still-circulating sample was dispersed by adding 10 mL of 50 g L^{-1} Na-MP to the beaker, then applying ultrasound with a probe immersed in the beaker (10.5 μm displacement setting) for 3 min. A final fully dispersed (FD) measurement was then made. For all measurements, the Mie optical model was used, with a refractive index of 1.55 (quartz) and an absorption of 0.1. Obscuration remained below 20% in most cases.

In every case, over the 180 min of continuous circulation, coarse (e.g. > 250 μm) size fractions generally decreased, while fine fractions, e.g. < 16 μm and < 2 μm, increased, indicating progressive disintegration of coarse silt- and sand-sized aggregates into finer aggregates or primary particles (Mason et al., 2011). These particle size trends are discussed in more detail in the Results section. We initially attempted to apply the equations used by Mason et al. (2011) to model increase of fine fractions, to the trends over time observed for the < 16 μm and < 2 μm fractions in this study, but satisfactory fits to the data could not be achieved. However, a similar approach proved successful, assuming two populations of aggregates with different stability and disintegration kinetics. The increase of < 16 μm and < 2 μm fractions were modeled using the following two equations:

$$\% < 16\,\mu m = A_{0,1}(1 - e^{-k_1 t}) + A_{0,2}(1 - e^{-k_2 t}) \quad (3)$$

$$\% < 2\,\mu m = A_{0,1}(1 - e^{-k_1 t}) + A_{0,2}(1 - e^{-k_2 t}) \quad (4)$$

where $A_{0,1}$ is the total percentage of the primary particles in each size fraction for aggregates that disintegrate rapidly, $A_{0,2}$ is the percentage of particles in the same size fraction for aggregates that disintegrate slowly, k_1 (for rapidly disintegrating aggregates) and k_2 (slowly disintegrating) are rate constants for aggregate disintegration, and t is circulation time in minutes. Typically, k_1 is about one order of magnitude larger than k_2. A_0 and k values were estimated using least squares, with R^2 typically > 0.95 for samples used in this study. No term for fine fraction content at $t = 0$ (e.g. C_2 in Eq. (1)) was found to be necessary. These equations predict that the content of < 16 μm or < 2 μm particles in the suspension asymptotically approaches $A_{0,1} + A_{0,2}$, but this is not necessarily the full content of these particle sizes in the sample that is released upon full dispersion. This reflects the fact that many samples appear to be approaching a steady state content of < 16 μm or < 2 μm particles during the experiment, and the estimated $A_{0,1}$ and $A_{0,2}$ values reflect this, but then substantial additional content of these particles is released with full dispersion. We used the < 16 μm fraction in Eq. (4) for exact comparison with other data from the same project, but results using the < 20 μm fraction would have been very similar.

2.4. Soil physicochemical characteristics

2.4.1. Soil texture

Previous work has shown that laser diffraction typically measures values of < 2 μm clay much lower than, and sometimes poorly correlated with, those obtained by the standard pipet method (e.g. Beuselinck et al., 1998; Mason et al., 2003). This does not affect our analyses involving comparison of particle size distributions that were all measured by laser diffraction; however, we also determined the clay content of all samples using the pipet method (Gee and Bauder, 1986), in order to test it as a predictor of aggregate behavior. Samples were pretreated with 30% H_2O_2 at 70 °C to oxidize organic matter, followed by dispersion with Na-HMP and shaking for 8 h.

2.4.2. OC and N content

The percentages of organic carbon (OC) and nitrogen (N) by mass were measured by combustion with a Thermo Scientific Flash 2000 NC Soil Analyzer. Samples with 1:1 water/soil pH values of ≥7.0 were assumed to potentially contain carbonate minerals, and were treated with fumes from concentrated HCl for up to 32 h to remove carbonates (Harris et al., 2001; Ramnarine et al., 2011).

2.4.3. Soil chemistry

Soil pH was measured using 1:1 water/soil mixtures by volume. Exchangeable bases were extracted using 1 M NH_4Oac adjusted to pH 7.0 to displace the bases from the soil samples (Thomas, 1982). The extracted base cations (Na^+, K^+, Ca^{2+}, and Mg^{2+}) were analyzed by ICP-OES at the University of Wisconsin Whitewater. Exchangeable acidity at the pH of the soil was measured by extraction with 1 M KCl followed by titration with NaOH (Thomas, 1982). The exchangeable bases plus exchangeable acidity was assumed to equal the effective

cation exchange capacity (ECEC) at the natural soil pH.

Cation exchange capacity (CEC) at pH 7.0 was measured by saturating exchange sites on soil colloidal surfaces with NH_4^+, then displacing the NH_4^+ into solution and measuring it using the Kjeldahl method (Black et al., 1965). Samples were shaken in 1 M NH_4Oac adjusted to pH 7.0, then let stand in this solution overnight. The samples were then filtered and rinsed with 50 mL 1 M NH_4Oac (pH 7.0), followed by an ethanol rinse to remove excess NH_4^+ that was not absorbed to the soil. The adsorbed NH_4^+ was then displaced from the soil sample with 120 mL acidified 10% NaCl, converted to NH_3 by a Kjeldahl distillation and titrated with $H_2SO_4^-$, with the displaced NH_4^+ assumed to represent total CEC.

Base saturation (BS) and effective base saturation (EBS) were calculated as the percentage of CEC or ECEC, respectively, occupied by exchangeable bases. For soils with pH ≤ 7.0 and some pH-dependent charge, CEC is generally greater than ECEC, and BS is less than EBS.

2.5. Statistical methods

For each sample, fitting Eqs. (3) and (4) to the observed changes in particle size distribution over 180 min yielded two values each for k_1 (rate constant for rapid aggregate disintegration) and k_2 (slower, later disintegration), one for the < 2 μm fraction and the other for the < 16 μm fraction. As noted in Section 2.3, the sum of the model parameters $A_{0,1}$ and $A_{0,2}$ in Eqs. (3) and (4) does not necessarily represent total < 16 μm or < 2 μm content in a sample, but these parameters are still likely to be dependent on sample texture. The ratio $A_{0,1}/A_{0,2}$, however, can be used as an index of the relative proportions of weak and strong aggregates over a wide range of textures. Besides these variables used in Eqs. (3) and (4), the ratio of the < 2 μm fraction or < 16 μm fraction in the FD measurement and in the final measurement taken before dispersion at 180 min (FD/180 min) is useful in indicating the relative abundance of especially stable aggregates that persist through 180 min of immersion in water and the mechanical stress of stirring and pumping.

To achieve the first objective of this study, we considered whether the distributions of k_1, k_2, $A_{0,1}/A_{0,2}$ and FD/180 min differ significantly between specific horizon types of Alfisols and Mollisols, using a Kruskal-Wallis test (nonparametric analysis of variance) followed by pairwise comparisons of distributions using Dunn's test with the Bonferroni *p*-value adjustment method (Dunn, 1964). To address the second objective, we investigated whether soil physicochemical characteristics are important controls on k_1, k_2, $A_{0,1}/A_{0,2}$ and FD/180 min, by testing linear models with predictor variables including CEC, ECEC, BS, EBS, pH, clay content, %OC, %N, and exchangeable Ca/Mg. The statistical analyses were carried out in R (RStudio Team, 2015), including the Dunn.test package (Dinno, 2017) and the *lm* (fit linear model) function.

3. Results[1]

3.1. Aggregate behavior

Experimental results can be visualized with plots of the change in the proportion of individual size fractions over time (Figs. 2, 3), or in continuous surface plots that portray change in the overall size distribution over time (Fig. 4). Fig. 2 portrays changes in size fractions for a single sample. The > 250 μm fraction includes macroaggregates, medium to coarse sand grains, larger coarse mineral fragments, roots, and other coarse organic fragments (the latter four constituents were not removed by sieving, to avoid crushing aggregates). This fraction declines rapidly in most samples, with at least half of the decline occurring in the first 20 min and almost all of it within 50 min, clearly reflecting disintegration of macroaggregates; the decline is followed by a relatively stable level, though in some cases with substantial fluctuation. The 50–250 μm fraction typically rises sharply to a peak in the first few minutes of circulation, then slowly declines, reflecting the initial rapid breakup of > 250 μm aggregates into smaller 50–250 μm aggregates, followed by slow disintegration of the latter into smaller aggregates and primary mineral particles. The short-term fluctuation of both of these coarse size fractions is probably due to a relatively small number of coarse organic fragments, aggregates, or sand grains that are not consistently picked up by the particle size analyzer pump and measured; given the small sample size, this can produce substantial fluctuations in the coarsest fractions.

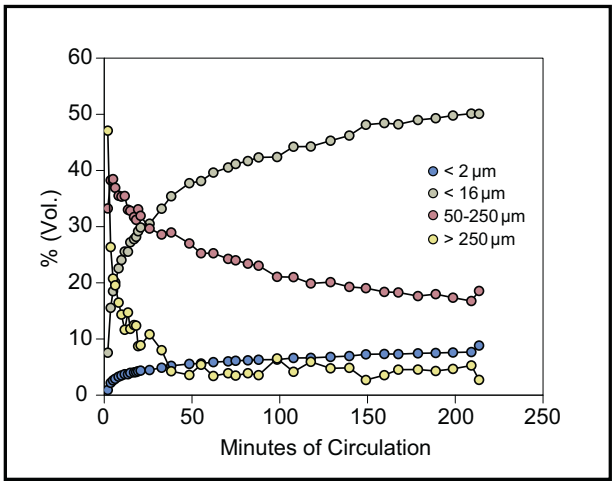

Fig. 2. Variations for multiple size fractions over the course of the experiment for an Alfisol (site: W-171 EA). Contents of the coarsest fractions (> 250 μm and 50–250 μm) decrease over time while finer fractions (< 16 μm and < 2 μm) increase over time.

In contrast, trends over time for the < 16 μm fractions are mostly smooth and monotonic, representing the increase in fine primary mineral particles (and possibly very fine aggregates) with greater circulation time. Trends for < 2 μm fractions are similar, but often somewhat noisier and sometimes displaying abrupt fluctuations. Because the data for these two finer fractions are less noisy and more conducive to quantitative analysis, we focus largely on them for the remainder of this paper. The term “fine material” used below refers to results applicable to both < 16 μm and < 2 μm fractions.

Experiments with A horizons of both Alfisols and Mollisols display a pattern in which initial aggregate disintegration and release of fine material is limited, with most released slowly over the course of the experiment (Fig. 3A). Plots of the > 250 μm fraction against time (e.g. Fig. 2) show that much of the initial release of fines comes from macroaggregates. The slow release of fines after ~50 min must come almost entirely from microaggregates, since the > 250 μm fraction has dropped to a stable level by that time. FD measurements reveal that a substantial portion of fine material is retained within the aggregates after 180 min of circulation. Mollisol A horizons generally show a steady rise in fine material content through the end of the experiment; Alfisol A horizons behave similarly but often appear to approach a plateau late in the analysis (Fig. 3A). Continuous surface plots provide insight on how the PSD as a whole changes over the 180 min of circulation (for clarity, FD measurements are not included in the distributions shown on these plots). Mollisol and Alfisol A horizons display a PSD dominated by a coarse peak (~100–200 μm) that is evident through the entire experiment, though its height slowly decreases over time (Fig. 4A). Particles that form this peak include primary sand grains, but many are highly stable aggregates; FD distributions show that a much smaller fraction of the samples is this coarse. The

[1] Sample IDs, soil physicochemical data, and full statistical results are reported in the Supplemental Material.

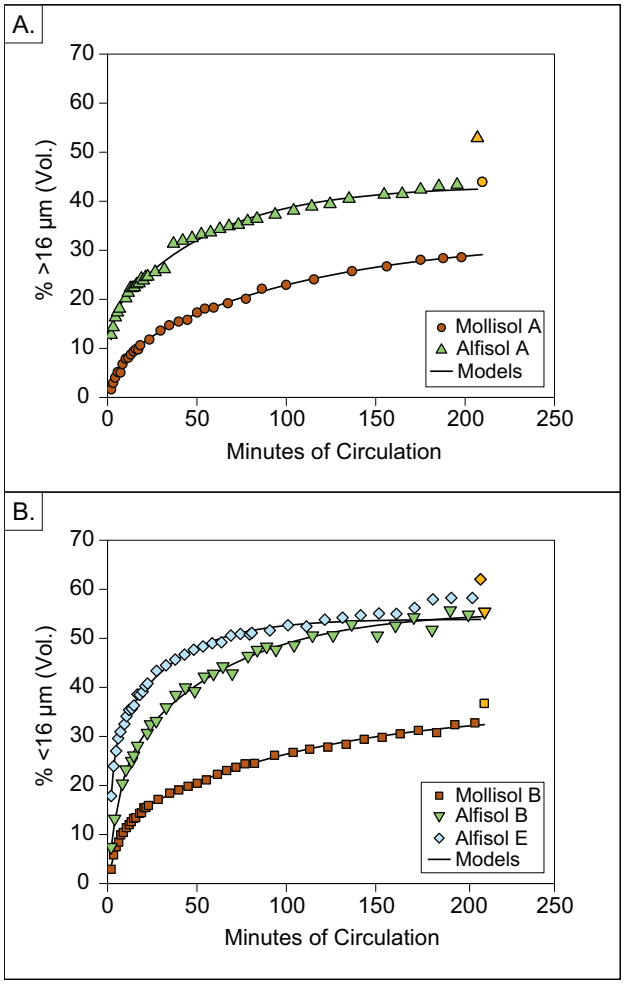

Fig. 3. Plots of the < 16 µm fraction released over time during the experiment, for different soil order and major horizon combinations. FD measurements are shown with same symbol but in gold for each series of measurements, and their shape corresponds to their respective soil order-horizon combination. (A) Mollisol and Alfisol A horizons (sites P-79 Ap1 and E-73 A, respectively); (B) Mollisol B, Alfisol E, and Alfisol B horizons (sites P-50 Bw, E-215 E, and E-133 Bt1, respectively). (For interpretation of the references to colour in this figure legend, the reader is referred to the web version of this article.)

persistence of this peak through the experiment indicates the relative stability of microaggregates—including many as large as 100–200 µm—in all of the A horizons.

In E horizons (present only in the Alfisols) aggregates disintegrate rapidly within the first few minutes of the experiment (Fig. 3B). Fine-material content quickly reaches a plateau, with little change through the rest of the 180 min. Very little additional fine material is released by full dispersion, that is, very few aggregates remain after the initial phase of rapid breakdown. Continuous surface plots of E horizons display a multimodal size distribution that develops rapidly (almost instantaneously in some cases), with dominant peak much finer (< 20 µm) than that observed in A horizons, a prominent secondary fine shoulder (~0.1 µm), and a poorly defined coarse shoulder (> 100 µm) (Fig. 4B). This pattern approximates the FD distribution, that is, it largely represents primary mineral particle sizes.

Mollisol B horizon samples show similar behavior to Mollisol A horizons (Fig. 3B), with limited rapid disintegration followed by a steady and slower disintegration, which does not plateau during the three-hour experiment. Mollisol B horizons, however, appear to have a smaller content of aggregates that persist for 180 min of circulation than do Mollisol A horizons, since they release less fine material at the point of full dispersion. A modal peak that persists through the experiment but diminishes in height indicating that it is formed at least partly of microaggregates is evident in continuous surface plots of Mollisiol B horizons (Fig. 4C). The diameter corresponding to this peak varies somewhat more in Mollisol B horizons than in Mollisol A horizons, corresponding to varying sand content in the FD distribution, which suggests microaggregates are not as important a component of the primary peak in the B horizons.

Alfisol B horizons display a large release of fine material at initial stages of the experiment, analogous to E horizons, but with at least some ongoing release of fines through the rest of the 3 h (Fig. 3B). The oscillation pattern displayed during intermediate stages of the experiment for the specific Alfisol B horizon shown here could be due to alternating dispersion and re-flocculation of clay particles released from aggregates. The early release of fine material is clearly displayed in the continuous surface plot in Fig. 4D. As with Mollisol B horizons, the dominant modal peak of the Alfisol B horizons varies, probably reflecting varying primary sand content. The sample shown in Fig. 4D displays a coarse shoulder (> 100 µm) that simultaneously becomes less well-defined and decreases in height over time, suggesting slow disintegration of relatively coarse microaggregates.

Some Alfisol E and B horizon samples yield FD measurements of the < 2 µm or < 16 µm fractions that are less than the final reading taken at 180 min, before dispersion. Mason et al. (2011) hypothesized that this is due to the instrument substantially underestimating the content of fine clay that is fully dispersed. That is, after 180 min of circulation much of the clay in these samples has likely been released from larger aggregates, but it is still not fully dispersed and exists in coarse clay- or fine silt-size aggregates, which are measured accurately, or at least not underestimated to the same extent as the fine clay. This interpretation implies that the < 2 µm and < 16 µm contents measured after full dispersion could be underestimated to some degree for all samples, even those from Mollisol A and B horizons, with FD fine material contents much higher than those measured before dispersion at 180 min. That is, it is likely that the FD/180 min ratio underestimates the true extent to which fine material is retained in stable aggregates through 180 min of circulation, though it is still a useful index of the relative content of highly water-stable aggregates.

3.1.1. *Effects of moisture content and reproducibility*

The two test samples analyzed in initially field-moist and air-dry conditions (Fig. 5A, B) included an A horizon and an E horizon from a forest site. The results demonstrate that initial moisture content can have a substantial effect on overall particle size trends and on the parameters k_1, k_2, $A_{0,1}/A_{0,\ 2}$, and FD/180 min. Furthermore, the nature of that effect may vary between horizons from the same site. Fine material content was greater throughout analyses for both horizons, indicating lower aggregate stability, when they were initially field moist rather than air-dry. For the A horizon sample (Fig. 5A), the best-fit values of k_1 and k_2 are very similar between analyses starting from field moist and air-dry conditions, but $A_{0,1}/A_{0,\ 2}$ is much higher and FD/180 min is lower for the initially field moist analysis. For the E horizon sample (Fig. 5B), there are somewhat larger differences of k_1 and k_2 between field-moist and air-dry analyses, but a smaller difference for $A_{0,1}/A_0$ and almost no difference for FD/180 min (these generalizations apply to both < 2 µm and < 16 µm fractions).

Replicate analyses of two samples suggest high reproducibility of the overall particle size trends for Alfisols and Mollisols (Fig. 5C, D). Variability of estimated parameters between replicates is substantial, but small compared to the significant differences of these parameters between horizon types of Mollisols and Alfisols (next section).

3.1.2. *Statistical analysis of differences in aggregate stability and disintegration rates*

As described in Section 2.5, we used parameters of the models described by Eqs. (3) and (4) (k_1, k_2, $A_{0,1}/A_{0,\ 2}$) and the ratio FD/180 min

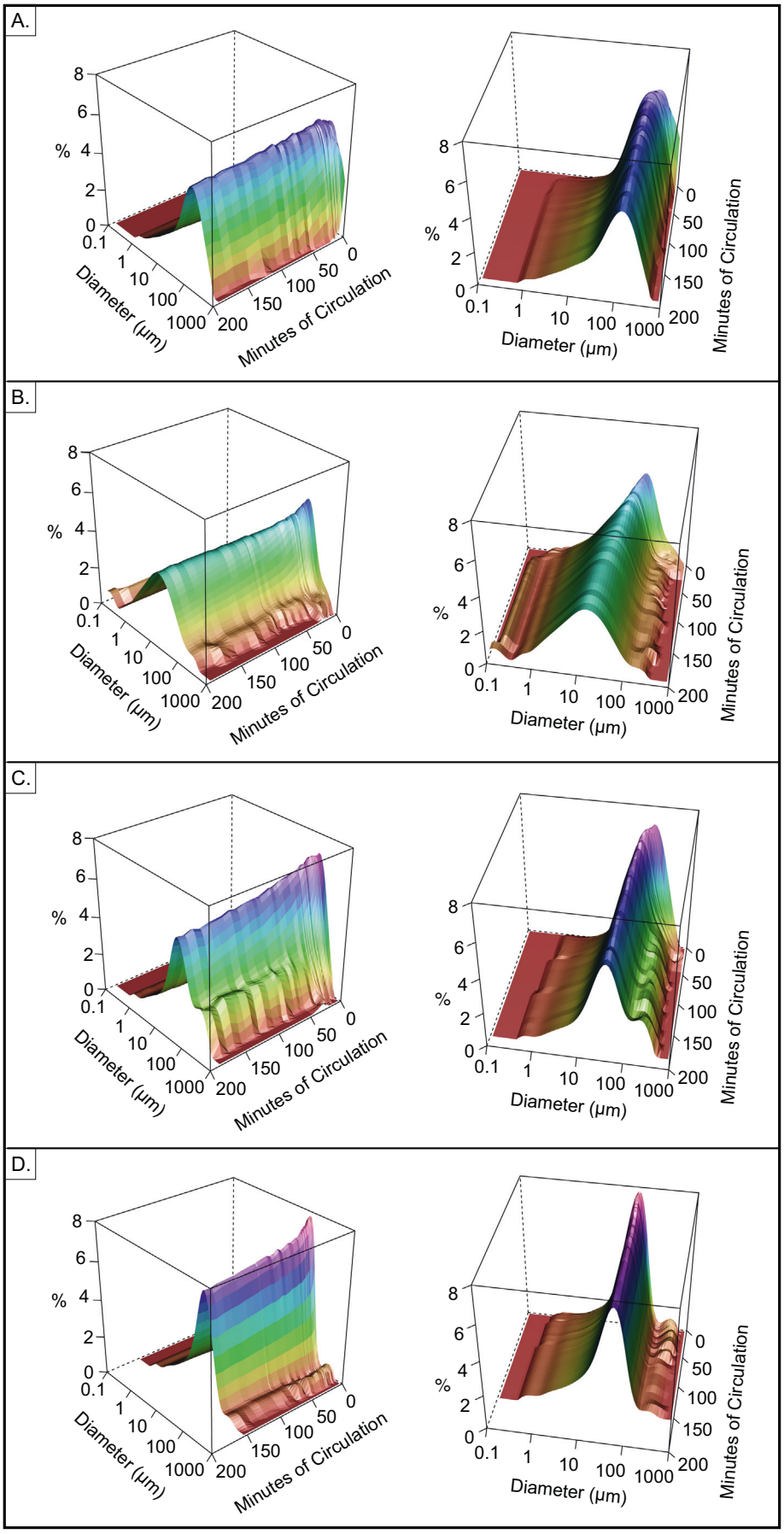

(caption on next page)

Fig. 4. Continuous surface plots of PSDs, for different soil orders and major horizon combinations. Height of surface represents relative abundance of each particle size class, as it changes over time from 0 to 180 min of circulation. (A) Mollisol A horizon (site W-22 A1); (B) Alfisol E horizon (site E-215 E); (C) Mollisol B horizon (site P-67 Bt1); (D) Alfisol B horizon (site E-73 BE).

to quantitatively differentiate and analyze aggregate behavior. Here we focus on how these parameters differ between samples from major horizons of Alfisols and Mollisols, using results for the < 16 μm fraction (Eq. (3)) only (descriptive statistics in Table 1). Kruskal-Wallis tests found that all four of these parameters vary significantly by soil order/horizon combination (Table 1).

Pairwise Dunn's tests found that for all parameters except k_2, the values estimated for Mollisol A horizons were drawn from significantly different distributions than those estimated for Alfisol E and B horizons (Table 1). Additional significant pairwise differences were found for individual parameters (see Table 1 for data supporting the following discussion). The k_1 value of a sample represents the rate of initial, rapid increase of fine material from weaker aggregates. Alfisol E horizons have by far the highest median value and largest interquartile range of k_1 of any of the major horizon types, while Mollisol A horizons have the lowest median k_1 values, indicating slow initial disintegration, followed by Mollisol B horizons; both of these have low interquartile ranges. Alfisol A and B horizons have similar median k_1 values, intermediate between those for Mollisol A and B horizons and those for E horizons. Besides the consistent difference between Mollisol A and Alfisol E and B horizons, Mollisol B horizon k_1 values are also drawn from a significantly different distribution than those for Alfisol E horizons.

All of the horizon types have relatively similar median values and interquartile ranges of k_2 (rate constant for the more stable aggregate pool, dominating the overall slow rate of rise in fine material late in the experiment), though the median is lowest for Mollisol A and B horizons. The only significant pairwise difference for k_2 is between Mollisol A and Alfisol B horizons.

Mollisol A and B horizons and Alfisol A horizons have relatively low values of $A_{0,1}/A_{0,2}$, with medians below 0.7, while Alfisol E and B horizons have higher values (> 1.0), indicating that more of the total fine material in the latter two horizon types is in aggregates that break down quickly in the early stages of the experiment. For $A_{0,1}/A_{0,2}$ there are numerous significant pairwise differences, between Mollisol A horizons and both E and B horizons of Alfisols, between Alfisol A horizons and E and B horizons of the same order, and between Mollisol B horizons and Alfisol E and B horizons.

Median values for FD/180 min are similar for Mollisol A and B horizons and Alfisol A horizons, between 1.3 and 1.5; these values well above 1.0 indicate substantial persistence of stable aggregates through 180 min of circulation. The ratios for Alfisol E and B horizons are much lower, close to or < 1.0, indicating almost complete disintegration of aggregates through circulation in water alone without chemical dispersion or sonication. Pairwise comparisons confirm that FD/180 min for Alfisol E and B horizons are drawn from significantly different distributions than both Mollisol A and B horizons and Alfisol A horizons.

3.2. Models for aggregate behavior as response to physicochemical soil characteristics

We tested a wide variety of linear models to predict k_1, k_2, $A_{0,1}/A_{0,2}$, and FD/180 min from soil properties including CEC, ECEC, %clay, % OC, %N, pH, BS, EBS, and exchangeable Ca/Mg. Models were tested for the entire dataset, and for the subsets of Mollisols, Alfisols, major horizon types (A, B, E), vegetation history zones (F1, F2, T, and P) (see Tables S3 and S4 in the supplementary information for full results including those not discussed here). Horizon types subdivided by soil order had low *n* and did not yield any significant models. Both the predictor variables and the parameters predicted were log-transformed

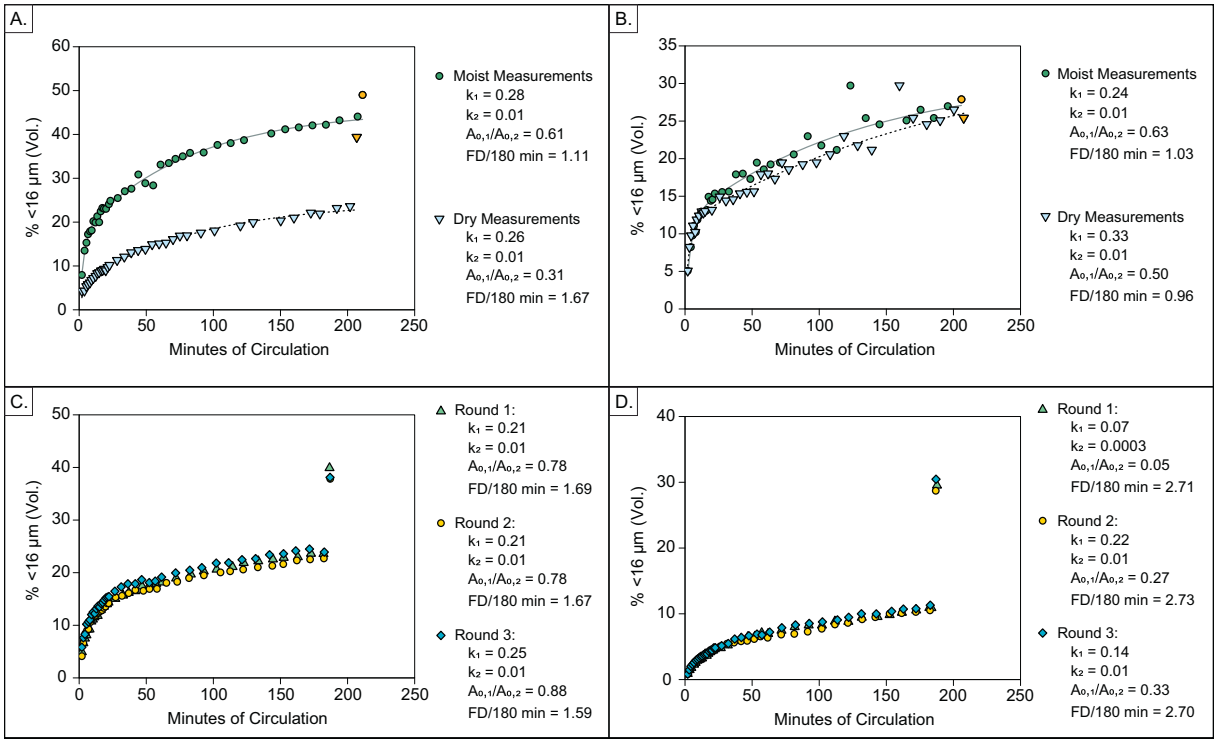

Fig. 5. Assessment of this method's sensitivity to initial moisture content and its overall reproducibility (both for the < 16 μm fraction). Parameters for Eq. (3) fit to each sample are included in the legends. (A) A horizon field-moist vs. air-dry conditions (site E-105 A); (B) E horizon field moist vs. air-dry conditions (site E-105 EA); (C) Replicate measurements for an Alfisol (site W-39 A); (D) Replicate measurements for a Mollisol (site P-98 A1).

Table 1
Descriptive statistics for aggregate stability parameters (Eq. (3)) by soil order/major horizon combinations, along with results of Kruskal-Wallis tests and pairwise comparisons of soil order/major horizon values using Dunn's test. For Kruskal-Wallis (K-W) tests, *p*-values < 0.05 are interpreted as indicating parameter values vary significantly by soil order/major horizon combination. For pairwise comparisons, *p*-values are for null hypothesis that samples from both pair members were drawn from the same distribution and are shown where < 0.05, interpreted as a significant difference between distributions.

k_1 (K-W $p < 0.0001$)				Pairwise comparison of distributions				
Soil horizons	1st Quartile	Median	3rd Quartile	Mollisol A	Mollisol B	Alfisol A	Alfisol E	Alfisol B
Mollisol A	0.107	0.120	0.159	X	–	–	$p < 0.0001$	$p < 0.05$
Mollisol B	0.161	0.164	0.207	–	X	–	$p < 0.05$	–
Alfisol A	0.197	0.271	0.333	–	–	X	–	–
Alfisol E	0.439	0.474	0.722	$p < 0.0001$	$p < 0.05$	–	X	–
Alfisol B	0.284	0.300	0.371	$p < 0.05$	–	–	–	X
k_2 (K-W $p < 0.01$)				Pairwise comparison of distributions				
Soil horizons	1st Quartile	Median	3rd Quartile	Mollisol A	Mollisol B	Alfisol A	Alfisol E	Alfisol B
Mollisol A	0.009	0.011	0.012	X	–	–	–	$p < 0.05$
Mollisol B	0.010	0.010	0.011	–	X	–	–	–
Alfisol A	0.011	0.013	0.016	–	–	X	–	–
Alfisol E	0.014	0.016	0.020	–	–	–	X	–
Alfisol B	0.015	0.016	0.018	$p < 0.05$	–	–	–	X
$A_{0,1}/A_{0,2}$ (K-W $p < 0.0001$)				Pairwise comparison of distributions				
Soil horizons	1st Quartile	Median	3rd Quartile	Mollisol A	Mollisol B	Alfisol A	Alfisol E	Alfisol B
Mollisol A	0.317	0.527	0.640	X	–	–	$p < 0.0001$	$p < 0.01$
Mollisol B	0.462	0.520	0.562	–	X	–	$p < 0.01$	$p < 0.05$
Alfisol A	0.568	0.652	0.803	–	–	X	$p < 0.05$	–
Alfisol E	1.014	1.167	1.751	$p < 0.0001$	$p < 0.01$	$p < 0.05$	X	–
Alfisol B	0.795	1.026	1.559	$p < 0.01$	$p < 0.05$	–	–	X
FD/180 min (K-W $p < 0.0001$)				Pairwise comparison of distributions				
Soil horizons	1st Quartile	Median	3rd Quartile	Mollisol A	Mollisol B	Alfisol A	Alfisol E	Alfisol B
Mollisol A	1.284	1.479	1.783	X	–	–	$p < 0.0001$	$p < 0.0001$
Mollisol B	1.423	1.457	1.503	–	X	–	$p < 0.05$	$p < 0.05$
Alfisol A	1.275	1.343	1.545	–	–	X	$p < 0.001$	$p < 0.001$
Alfisol E	0.904	0.953	1.017	$p < 0.0001$	$p < 0.05$	$p < 0.001$	X	–
Alfisol B	0.886	0.927	1.063	$p < 0.0001$	$p < 0.05$	$p < 0.001$	–	X

because this yielded approximately linear relationships in some cases and because the predicted parameters were not normally distributed (based on the Shapiro-Wilks test) before transformation. The resulting models are power-law relationships between the untransformed variables. All models were fit using least squares. Here we mainly discuss models for the $< 16\,\mu m$ fraction, significant at $p < 0.05$, for which $R^2 \geq 0.33$. Important cases where results differ for the $< 2\,\mu m$ fraction are briefly noted. No models using more than one predictor variable performed better than those with one predictor, based on adjusted R^2 and the Akaike Information Criterion (Akaike, 1973), so only the latter are considered here.

CEC, ECEC, %OC, and %N were by far the most common predictor variables for k_1 and FD/180 min, in models with $R^2 \geq 0.33$. Models for k_1 involve negative relationships with those variables, i.e. greater tendency for early, rapid aggregate disintegration with decreasing CEC, ECEC, %OC, and/or %N (Fig. 6, Table 2). Models for FD/180 min involve positive relationships, indicating greater content of stable aggregates that persist to the end of the experiment with increasing CEC, ECEC, %OC, and/or %N (Fig. 7, Table 2).

Both CEC and ECEC clearly emerged as the most broadly applicable predictors of k_1 ($< 16\,\mu m$). Models using those predictors were significant and had $R^2 \geq 0.33$ for all samples, for Alfisols alone, for E horizons, and for F2 soils; a significant model was also identified for T soils using ECEC but not CEC (Fig. 6A–D). The relationships for F2 soils are the strongest of these models ($R^2 = 0.59$ for CEC, $R^2 = 0.50$ for ECEC). Models using %OC to predict k_1 ($< 16\,\mu m$) were significant, with $R^2 \geq 0.33$ only for E horizons, though a model with $R^2 = 0.32$ was identified for F2 soils (Fig. 6E). Using %N as a predictor of k_1 ($< 16\,\mu m$) produced significant models with $R^2 \geq 0.33$ for E horizons, F2 soils, and T soils (Fig. 6F). Modeling k_1 ($< 2\,\mu m$) yielded similar results, though with moderately higher R^2 in some cases and with %N as an additional predictor for the whole sample set and for Alfisols (not shown).

In contrast to the case with k_1 ($< 16\,\mu m$), CEC and ECEC do not emerge as predictors of FD/180 min ($< 16\,\mu m$) at all. Significant models with $R^2 \geq 0.33$ instead involved relationships with %OC, %N, BS, and/or exchangeable Ca/Mg, often fairly weak. (Fig. 7, Table 2). FD/180 min ($< 16\,\mu m$) is positively related to %OC for Alfisols, F1 soils, and F2 soils, with $R^2 \geq 0.33$ and as high as 0.71 for the F2 subset (Fig. 7A,B; a significant model for the whole dataset had $R^2 = 0.31$. Models for FD/180 min ($< 16\,\mu m$) using %N as a predictor were significant for all samples, Alfisols, F1, F2, and T soils, with particularly high R^2 for F1 and F2 subsets (Fig. 7C, D). FD/180 min ($< 16\,\mu m$) is positively related to BS or Ca/Mg in significant models identified for a few subsets (E horizons, B horizons, F2 soils; Fig. 7E, F). FD/180 min ($< 2\,\mu m$) is positively related to BS for E horizons, and to CEC, %N, and %OC for F2 soils (not shown).

Few models with $R^2 \geq 0.33$ could be developed for either k_2 or $A_{0,1}/A_{0,2}$ ($< 16\,\mu m$ or $< 2\,\mu m$), either for the whole dataset or subsets. Those that were identified involve negative relationships of k_2 with Ca/Mg, pH or clay, positive relationships of $A_{0,1}/A_{0,2}$ with Ca/Mg, ECEC, or CEC, all for individual subsets (Tables S3 and S4 in the supplemental information).

A final noteworthy observation is that significant predictive models could not be identified for any of the parameters for the overlapping subsets of Mollisols, A horizons, or P soils (Table 2). Thus, variation *within* those subsets could not be explained by the physicochemical characteristics we tested as predictors, despite the distinctive behavior of their aggregates relative to other subsets.

4. Discussion

4.1. Pedogenic aggregate behavior

The results of this study demonstrate that the method developed by Mason et al. (2011) for assessing sedimentary aggregate stability can

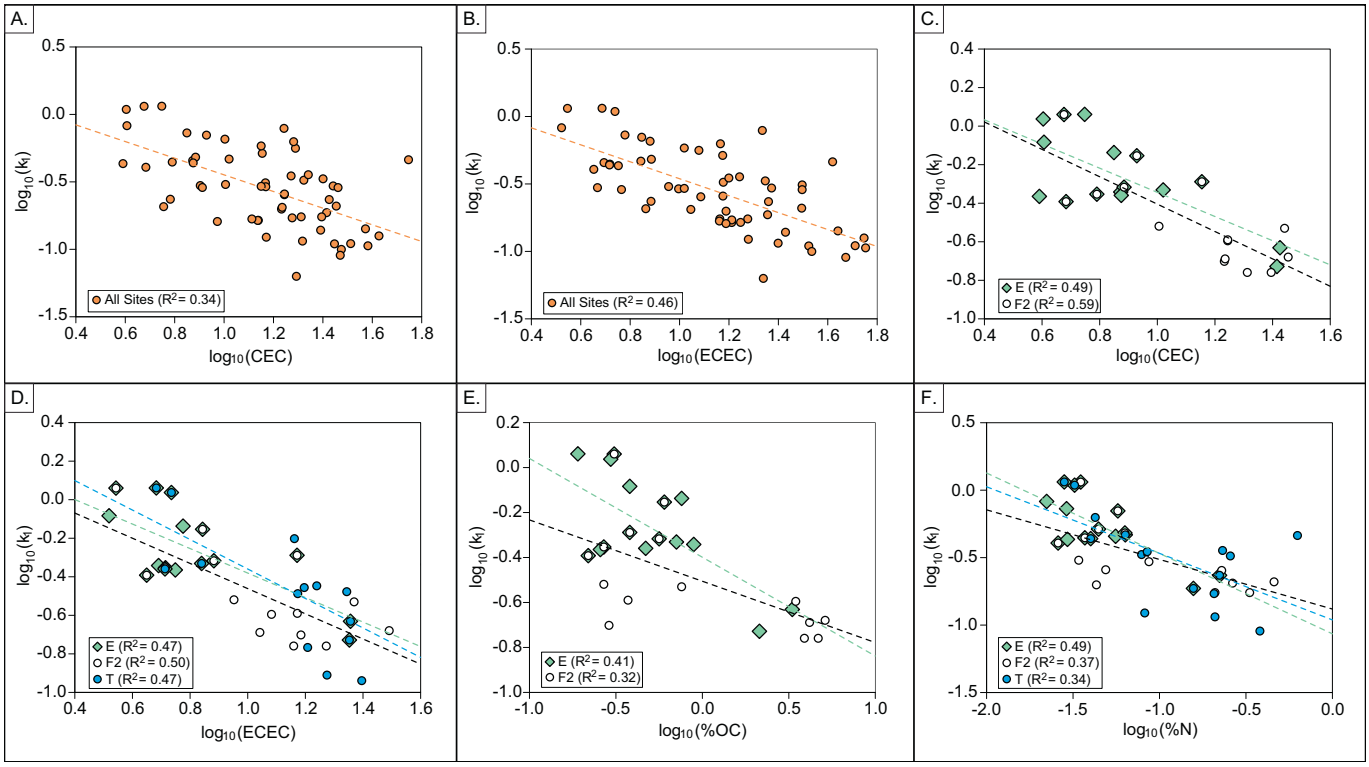

Fig. 6. Best-fit simple linear regression models predicting k_1 from physicochemical soil characteristics. All variables have been log-transformed in order to approach normal distributions. (A) CEC for all samples; (B) ECEC for all samples; (C) CEC for E horizons and F2 soils; (D) ECEC for E horizons, F2 soils, and T soils; (E) %OC for E horizons and F2 soils; (F) %N for E horizons, F2 soils, and T soils.

also provide valuable information on pedogenic aggregate behavior. Plots of fine material increase over time and continuous surface plots of overall change in the PSD both reveal large differences between samples, in terms of aggregate disintegration rates and content of persistent, water-stable aggregates. These plots bring out the particularly large contrast between E horizons and the A horizons of both Mollisols

Table 2
Simple linear regression results for < 16 μm fraction, models predicting k_1 and FD/180 min from physicochemical properties for all samples and subsets (all variables log-transformed). Symbols next to adjusted R^2 indicate significance level.

Samples	k1						FD/180 min					
	Variable	Slope	Intercept	Std. error	Adj. R^2	AIC	Variable	Slope	Intercept	Std. error	Adj. R^2	AIC
All (n = 59)	ECEC	−0.63	0.17	0.23	0.46****	−7.51	%OC	0.14	0.06	0.10	0.31****	−98.26
	CEC	−0.62	0.17	0.24	0.34****	4.36	%N	0.18	0.26	0.10	0.35****	−102.30
Alfisols (n = 40)	ECEC	−0.51	0.09	0.19	0.34****	−15.03	%OC	0.13	0.03	0.08	0.41****	−87.19
	CEC	−0.50	0.13	0.19	0.35****	−15.60	%N	0.17	0.22	0.07	0.48****	−91.94
							Ca/Mg	0.36	−0.18	0.08	0.33****	−82.02
Mollisols (n = 19)	No significant relationships						No significant relationships					
A horizons (n = 27)	No significant relationships						No significant relationships					
E horizons (n = 16)	ECEC	−0.64	0.26	0.16	0.47**	−8.53	BS	0.18	0.001	0.04	0.43**	−58.11
	CEC	−0.63	0.28	0.16	0.49**	−9.00						
	%OC	−0.44	−0.40	0.17	0.41**	−6.65						
	%N	−0.60	−1.07	0.16	0.49**	−9.16						
B horizons (n = 16)	No significant relationships						Ca/Mg	0.66	−0.27	0.09	0.41**	−29.09
Prairie (n = 16)	No significant relationships						No significant relationships					
Transition (n = 16)	ECEC	−0.77	0.41	0.24	0.47**	3.01	%N	0.23	0.26	0.11	0.42**	−22.19
	%N	−0.49	−0.96	0.26	0.34*	6.54						
Forest 2 (n = 15)	ECEC	−0.65	0.19	0.17	0.50**	−6.97	%OC	0.17	0.06	0.06	0.71****	−39.96
	CEC	−0.71	0.31	0.15	0.59***	−9.84	%N	0.21	0.27	0.06	0.66***	−37.46
	%OC	−0.27	−0.51	0.20	0.32*	−2.31	Ca/Mg	0.42	−0.20	0.08	0.44**	−30.03
	%N	−0.37	−0.88	0.19	0.37*	−3.28						
Forest 1 (n = 12)	No significant relationships						%OC	0.15	0.06	0.08	0.44*	−23.97
							%N	0.22	0.31	0.06	0.62**	−28.82
							pH	1.26	−0.86	0.08	0.31*	−21.55

* $p < 0.05$.
** $p < 0.01$.
*** $p < 0.001$.
**** $p < 0.0001$.

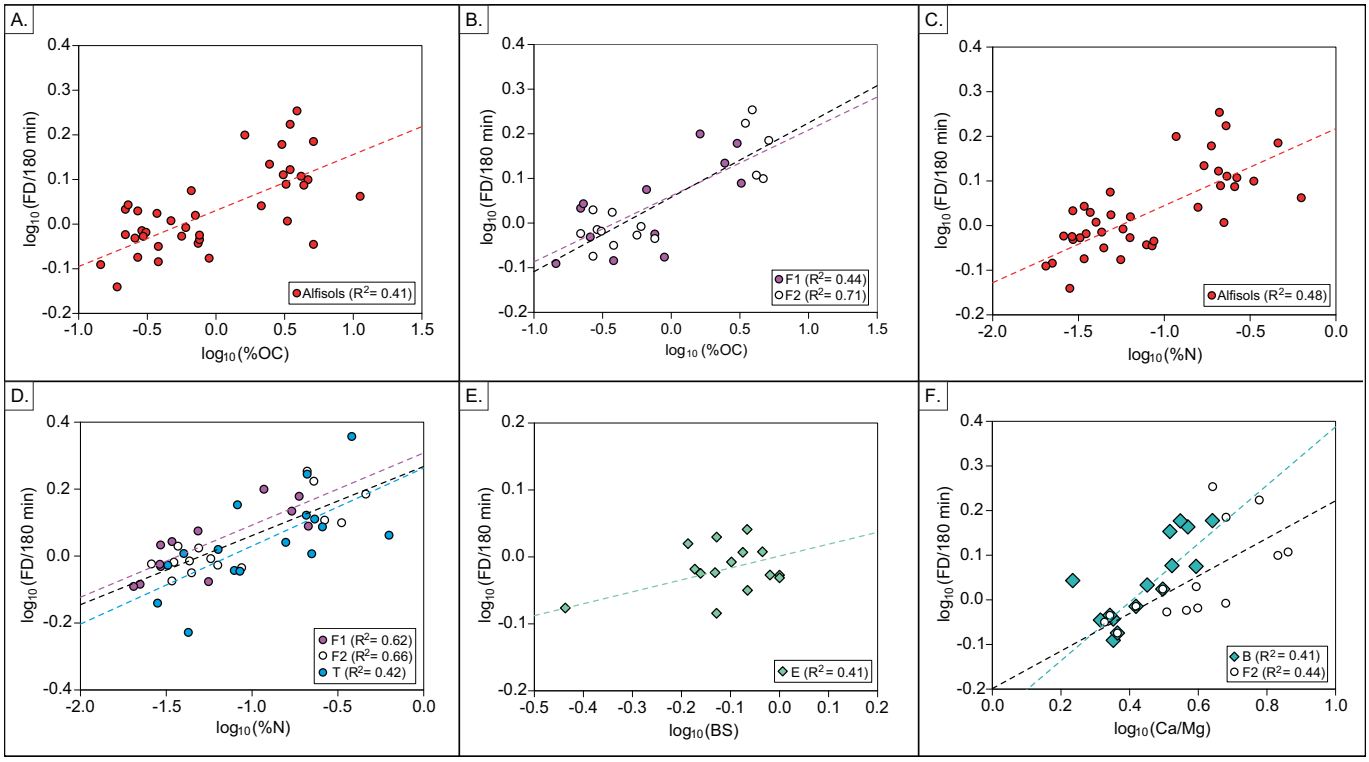

Fig. 7. Best-fit simple linear regression models predicting FD/180 min ratios from physicochemical soil characteristics. All variables have been log-transformed. (A) %OC for Alfisols; (B) %OC for F1 soil, and F2 soils,; (C) %N for Alfisols, (D) %N for F1 soils, F2 soils, and T soils, (E) Base Saturation for E horizons; (F) Ca/Mg for B horizons and F2 soils.

and Alfisols, while other differences are more subtle but still evident. It is worth noting that the trends in particle size fractions as a function of circulation time, observed in this study, are quite similar in form to trends observed as a function of energy applied by ultrasound in the study of Fristensky and Grismer (2008), suggesting that both approaches provide similar information on the dynamics of aggregate breakdown.

The rapid early release of fines, especially from E horizons but to some extent even in Mollisol A horizons, is consistent with an important role for slaking of aggregates in the first stages of these experiments. The ongoing release of fine material, but at progressively lower rates over time, would then reflect increasing predominance of differential swelling, physicochemical dispersion, and mechanical stress as mechanisms of aggregate disintegration. To some extent, this transition in disintegration process may explain why the assumption of two aggregate populations in Eqs. (3) and (4) fits most of the experimental data so well. The almost complete loss of macroaggregates within the first 20–50 min suggests a high susceptibility to slaking and is consistent with the hierarchy of aggregate size and stability first described by Tisdall and Oades (1982). The persistence of a slowly declining primary mode, > 50 μm in many A and B horizon samples, makes it clear that some relatively large microaggregates remain through much or all of the experiment (Fig. 4).

By modifying the approach of Mason et al. (2011) to include an assumption of two aggregate populations, first-order rate law models provided a good fit to observed aggregate disintegration over time, in most cases. The parameters estimated for these models can be related to soil morphology in many cases. In particular, Mollisol A horizons with relatively slow aggregate disintegration and abundant stable aggregates have significantly lower k_1, lower $A_{0,1}/A_{0,2}$, and higher FD/180 min than E horizons. Alfisol A horizons have median values of k_1, $A_{0,1}/A_{0,2}$, and FD/180 min that are similar to those of Mollisol A horizons but offset somewhat in the direction of lower aggregate stability. This observation is consistent with moderately faster disintegration of aggregates in many Alfisol A horizons relative to those of Mollisols. Alfisol B horizons are relatively close to E horizons in their behavior, except for their lower k_1 values, and they also significantly differ from Mollisol A horizons for most parameters. Mollisol B horizons have behavior closer to that of Mollisol or Alfisol A horizons than to the Alfisol B horizons; they are not significantly different from either group of A horizons for any parameter, but they do differ significantly in some cases from Alfisol B and E horizons.

Based on these observations and the data collected on soil physicochemical properties, the most obvious explanation for differences in aggregate behavior involves OM content, though other possible factors are also apparent. Mollisol A horizons have high OM content relative to most other soil horizons sampled in this research, clearly suggesting that OM could explain their relatively slow aggregate disintegration and high stable aggregate content. Alfisol A horizons also have relatively high OM content, but could possibly have different OM composition, affecting their behavior. Mollisol A horizons also have BS and EBS of ~100% and four out of 14 of them have pH > 7.0 (data not shown), suggesting the presence of carbonate minerals. Both of these properties imply an abundant supply of Ca^{2+} and Mg^{2+}, limiting clay dispersion and stabilizing aggregates. In contrast, while Alfisol A horizons have EBS near 100%, their BS is often somewhat lower and their pH is always < 7.0, possibly explaining their somewhat different behavior.

The behavior of E horizons, with rapid disintegration and few persistent stable aggregates, is consistent with a major role for OM, since these horizons are OM-poor. The E horizons in this study also generally have lower BS than all Mollisol A horizons, and relatively low clay content, both of which could reduce aggregate stability. Mollisol and Alfisol B horizons displayed surprisingly different behavior. Mollisol B horizons have much higher FD/180 min ratios; while Alfisol B horizons have similar k_1 values to Alfisol A horizons, their FD/180 min values are similar to those of Alfisol E horizons. The B horizons of both soil orders have similarly low OM content, and have a wide range of clay

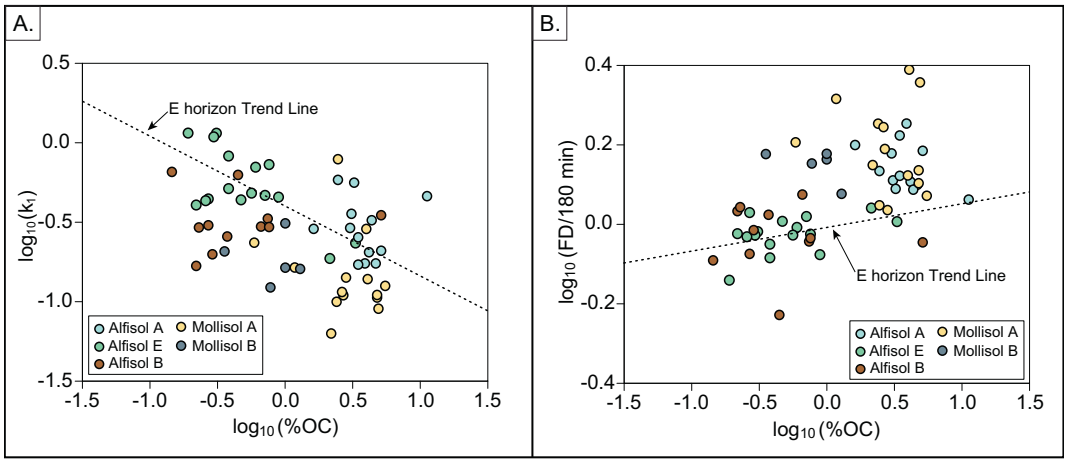

Fig. 8. Scatterplots of %OC vs. parameters of Eq. (3), for samples from different soil order/major horizon combinations. Trend lines representing significant but weak relationships for E horizons are displayed as a reference for discussion in the text on lack of significant relationships for other subsets or all samples combined. (A) k_1 values; (B) FD/180 min ratios.

contents. Mollisol B horizons have BS of ~100% and three out of six of these horizons have pH > 7.0, however. Most Alfisol B horizons have pH < 6.0 and BS < 85%, probably increasing the likelihood of clay dispersion and aggregate disintegration.

4.2. Interpretation of linear modeling results

Given the observed trends between soil order and horizon types, it is initially somewhat surprising that %OC did not emerge as the most important predictor of the parameters of Eqs. (3) and (4) or of FD/180 min, and BS was only rarely identified as a predictor at all. Instead, ECEC and CEC were most often identified as predictors of one parameter (k_1), usually in models with relatively low R^2, while similar weak relationships with %OC and %N are mainly evident in models of k_1 and FD/180 min for certain subsets, especially E horizons, F2 soils, and T soils.

Scatterplots provide some insight into why there are not clearer relationships of k_1 or FD/180 min with %OC for the whole dataset (Fig. 8). In the case of k_1, E horizons display a linear relationship between that variable and %OC (Fig. 6E). Alfisol and Mollisol A horizons have k_1 values roughly consistent with that relationship, but Alfisol A horizons tend to have higher k_1 values (more rapid early breakdown) than do Mollisol A horizons with similar %OC. This difference, weakening the relationship of k_1 with %OC for the whole dataset, may reflect a difference in organic matter composition. The Alfisol A horizons often contain abundant coarse organic fragments, typical of forest soils (Adu and Oades, 1978; Mikutta et al., 2007), which contribute to %OC but add little to aggregate stability. Alfisol and Mollisol B horizons both have relatively low k_1 values (less rapid early breakdown), falling below the %OC-k_1 trend of E horizons (Fig. 8A). In Alfisol B horizons, this slower breakdown may be attributable to high clay content, while in Mollisol B horizons it could be explained by the presence of carbonates and abundant exchangeable Ca^{2+}.

In the case of FD/180 min ratios, Alfisol and Mollisol A horizons have the highest FD/180 min ratios, and generally fall well above the %OC-FD/180 min trend of E horizons (Fig. 8B). It is possible that processes more active in A horizons, such as fine root growth and soil faunal activity, may add to the aggregate stability provided by OM. Mollisol B horizons also fall above the E horizon trend, but have lower %OC than that of A horizons; in this case, persistent stable aggregates may reflect the presence of carbonates and abundant exchangeable Ca^{2+}, as with k_1. Alfisol B horizons appear to fall along the roughly the same trend as E horizons, indicating both have similar aggregate strength and OC content. F1 and F2 soils display a linear relationship with %OC (Fig. 7B). P soils (all Mollisols) do not follow this trend at all however, and for horizons in the mid- to low-%OC range (mostly B horizons), P soil horizons have higher FD/180 min than F1, F2, and T soil horizons. Again, this observation likely reflects the stabilizing effect of carbonates and exchangeable Ca^{2+} (the P soils are all Mollisols).

Given the frequency with which ECEC and/or CEC emerge as predictors of all of the parameters, it is important to consider the potential complexity in this relationship. Both ECEC and CEC are determined by multiple physicochemical soil characteristics (e.g. pH, clay mineralogy and content, and OM) which to some extent can substitute for, or offset, each other. Using data from the samples analyzed here and additional horizons from the same soils, Kasmerchak (2016), found that much of the variance in CEC can be explained by the model:

$$\mathrm{CEC} = 1.12 + 3.54(\%\mathrm{OC}) + 0.53(\%\mathrm{Clay})$$
$$n = 83,\ R^2 = 0.81 \quad (5)$$

The variance not explained by this model may in part represent other factors such as clay mineralogy. For ECEC, pH is also an important factor, but this property will still be strongly related to OC and clay content. Eq. (5) implies that a sample with low clay content but high OC may have a similar CEC to one with higher clay content but low OC. Greater content of clay minerals with high CEC might similarly offset low OC. Thus, the relationships with CEC and ECEC that we found could actually represent underlying dependence of aggregate stability and disintegration rates on OC and clay content, and possibly clay mineralogy, which are not evident because of these interactions. In theory, a more complex multivariate model could represent such multiple controls and their interactions, but none we tested performed well at all.

The observation that models using %N as a predictor explained more variance than those using %OC in some cases is enigmatic. Most N in these soils is likely to be in organic matter, so N and OC are correlated, though the C:N ratio increases with depth (unpublished data, J. Mason). Thus, it may simply be a matter of chance that the weak relationships of aggregate stability parameters with %N are sometimes a little stronger than those with %OC. It is also possible that the relationships with %OC for some samples are weakened by abundant coarse fragments of minimally decomposed organic matter, which contribute less to aggregate stability than more N-rich humified organic matter.

Regardless of the explanations for specific unexpected results of this effort to relate aggregate stability parameters with soil physicochemical properties, even the more successful models rarely explain more than half of the variance. We suggest that this result reflects the limitations

of such models in representing the many complex factors and processes that influence aggregate development and stability in forest and grassland ecosystems. The properties we considered are no doubt influential, but the models do not incorporate differences in soil faunal activity, root density, or root exudates associated with specific plant species, for example.

4.3. Relationships of aggregate stability and pedogenesis under forest and grassland

In many ways, the most conclusive quantitative results of this study involve the clear differences between aggregate stability parameters (k_1, $A_{0,1}/A_{0,2}$, and FD/180 min) associated with specific horizons of Alfisols and Mollisols. These results demonstrate that pedogenesis under forest and grassland ecosystems produces soil profiles differing in aggregate behavior, as well as more obvious differences of organic matter content and A to B horizon textural contrast. The thick, OM-rich A horizons of Mollisols stand out because of their slowly disintegrating, often highly water-stable aggregates. The underlying B horizons also have at least moderately abundant stable aggregates, possibly related to carbonate content. In contrast, Alfisols have profiles with thinner A horizons with relatively stable aggregates overlying E horizons with minimally stable aggregates, and B horizons with some relatively persistent aggregates, likely due to higher clay content.

These contrasting profiles can potentially be explained by differences in predominant processes in forest and grassland ecosystems. The deep OM-rich A horizons of Mollisols can be attributed to the relative importance of belowground OM additions under grasslands (Parton et al., 1987; Tisdall, 1996), while predominance of surface additions under forest can explain much thinner A horizons underlain by OM-poor E horizons. Despite the difficulty we found in demonstrating a strong effect of %OC on aggregate stability through linear modeling, abundant previous research supports an important role for OM in formation of stable aggregates. Other differences between forest and grassland ecosystems that we did not try to model could also play important roles. These include differences in root distribution and in the frequency and type of burrowing and other soil faunal activity and disturbance (e.g. Hole, 1981; Johnson et al., 1987; Schaetzl, 1986), which both lead to very different soil OM profiles than those under forest (Schaetzl and Thompson, 2015). Additionally, the depletion of Ca^{2+} from subsurface horizons through root uptake and deposition on the soil surface in litterfall (Lawrence et al., 1995; Attiwill, 1968), could in theory decrease formation of stable aggregates in Alfisol E horizons by reducing the potential for Ca^{2+} bridging between organic matter and mineral surfaces (Oades, 1984, 1988, 1993; Mikutta et al., 2007; von Lutzow et al., 2007, 2008).

The results of our aggregate stability experiments, interpreted in terms of contrasting pedogenic processes under forest and grassland, also provide important information on how the soils in the study area may have changed following forest invasion of grassland. Reduced belowground input of OM and a decline in OM content over time below a thin A horizon, would have ultimately reduced the stability of aggregates in subsurface horizons; changes in soil faunal activity and uptake of Ca^{2+} would have also reduced their stability. This in turn could have led to an increase in downward clay translocation, and ultimately allowed texture-contrast profiles to develop. Following initial clay mobilization, the remaining clay content in the emerging E horizon would have been lower, perhaps further weakening any remaining aggregation, and thus acting as a positive feedback on clay translocation to the B horizon. Any clay added to the E horizon, for example by bioturbation, would have then been more easily eluviated from it.

4.4. Potential for application to studies of soil erosion and response to land use change

We did not explore the applicability of the aggregate analysis method used here to studying connections between land management practices, soil structure, surface seal formation, infiltration, and erosion, but the potential for this type of application seems clear. For example, results of this study suggest that conversion of our sampling sites to row crop agriculture could have different impacts in terms of the subsequent runoff and erosion rates, depending on soil order and vegetation history. That is, the slow initial aggregate breakdown, and abundance of water-stable aggregates, in Mollisol A horizons, suggests they would behave differently under direct exposure to rainfall than a plow layer made up of thin Alfisol A horizons, mixed with E horizons with minimal aggregate stability. This hypothesis could be tested using field experiments with rainfall simulation, which more broadly is the best approach for relating results of the method described here to behavior of a soil in the field.

5. Conclusions

The method of Mason et al. (2011), using laser diffraction to monitor aggregate disintegration during 3 h of circulation in water, clearly identified contrasts in pedogenic aggregate stability and disintegration rates among soils formed under grassland and forest. The model used by Mason et al. (2011) to represent fine material released by aggregate breakdown as a first-order process (Field and Minasny, 1999) did have to be modified, however, to include two aggregate populations with different disintegration rates. The most stable aggregates and lowest initial rates of disintegration were observed in A horizons, particularly those of Mollisols formed under grassland. Aggregates in E horizons of Alfisols formed under forest (or a sequence of grassland followed by forest) were the least stable and rapidly released most of the internally-bound fine material. Mollisol B horizons were also relatively stable, whereas Alfisol B horizons behaved similarly to E horizons, but with somewhat slower breakdown and evidence for some persistent water-stable aggregates. The behavior displayed in these experiments suggested a strong influence of OM and exchangeable bases on aggregate stability, since the Mollisols A horizons have high OM and Mollisol B horizons often have high pH and BS of ~100%, while Alfisol E horizons have low OM and along with Alfisol B horizons often have lower pH and BS.

Linear modeling did identify %OC and %N as a predictor of parameters representing aggregate disintegration rate and highly water-stable aggregate content in some cases, for some subsets of soils. Other soil properties, especially ECEC or CEC, were more often identified as predictors of those parameters, however. Both ECEC and CEC may indirectly represent effects of OM and clay content, both of which are thought to influence aggregate stability and either of which can be the most important contributor to ECEC and CEC in a particular horizon. Overall, linear modeling suggested that it is difficult to explain the contrasting behavior of aggregates in different soil horizons using simple lab-measured physicochemical properties.

The results of this study help explain the transformation of soil morphology after forest invaded grassland over the past 4000 years in the study area, particularly the development of texture-contrast profiles. The method of aggregate analysis used here may also be valuable in research on soil response to changes in land cover or management, though we did not explore that possibility.

Acknowledgements

Research funded by the National Science Foundation, Geography and Spatial Sciences Program grant BCS-1263582. We thank Laura Eddy, Adam Jannke, Hawa Keita, Fei Ma, and Zhiwei Xu for field and lab assistance. Numerous landowners, the Minnesota DNR, and the Chippewa National Forest provided access to study sites.

Appendix A. Supplementary data

Supplementary data to this article can be found online at https://doi.org/10.1016/j.geoderma.2018.06.020.

References

Adu, J.K., Oades, J.M., 1978. Physical factors influencing decomposition of organic materials in soil aggregations. Soil Biol. Biochem. 10, 109–115.

Akaike, H., 1973. Information theory and the maximum likelihood principle in *2nd International Symposium on Information Theory*. In: Petrov, B.N., Cs ä ki F (Eds.), Akademiai Ki à do, Budapest.

Almajmaie, A., Hardie, M., Acuna, T., Birch, C., 2017. Evaluation of methods for determining soil aggregate stability. Soil Tillage Res. 167, 39–45.

Almendinger, J., 1990. The decline of soil organic matter, total-N, and available water capacity following the Late-Holocene establishment of jack pine on sandy Mollisols, north-central Minnesota. Soil Sci. 150, 68–694.

Amézketa, E., 1999. Soil aggregate stability: a review. J. Sustain. Agric. 14, 83–151.

Attiwill, P.M., 1968. Loss of elements from decomposing litter. Ecology 49, 142–145.

Bartlein, P.J., Webb III, T., Fleri, E., 1984. Holocene climate change in the northern Midwest: pollen-derived estimates. Quat. Res. 52, 388–392.

Beuselinck, L., Govers, G., Poesen, J., Degraer, G., Froyen, L., 1998. Grain-size analysis by laser diffractometry: comparison with the sieve-pipette method. Catena 32, 193–208.

Bieganowski, A., Ryzak, M., Witkowska-Walczak, B., 2010. Determination of soil aggregate disintegration dynamics using laser diffraction. Clay Miner. 45, 23–34.

Black, C.A., Evans, D.D., White, J.L., Ensminger, L.E., Clark, F.E., 1965. Methods of Soil Analysis Part 2: Chemical and Microbiological Properties. American Society of Agronomy Inc., Madison WI.

Bradbury, J.P., Dean, W.E., Anderson, R.Y., 1993. Holocene climatic and limnologic history of the north-central United States as recorded in the varved sediments of Elk Lake, Minnesota; a synthesis. In: Bradbury, J.P., Dean Walter, E. (Eds.), Elk Lake, Minnesota; Evidence for Rapid Climate Change in the North-central United States. Geological Society of America (GSA), Boulder, CO, United States, pp. 309–328.

Brugam, R.B., Grimm, E.C., Eyster-Smith, N.M., 1988. Holocene environmental-changes in Lily Lake, Minnesota inferred from fossil diatom and pollen assemblages. Quat. Res. 30, 53–66.

Buell, M., Cantlon, J., 1951. A study of two forest stands in Minnesota with an interpretation of the prairie-forest margin. Ecology 32, 294–316.

Buurman, P., Pape, T., Muggler, C.C., 1997. Laser grain size determination in soil genetic studies: 1. Practical problems. Soil Sci. 162, 211–218.

Clark, J., Grim, E., Lynch, J., Mueller, P., 2001. Effects of holocene climate change on the c4 grassland/woodland boundary in the Northern Plains. Ecology 82, 620–636.

Clement, C.R., Williams, T.E., 1958. An examination of the methods of aggregate analysis by wet sieving in relation to the influences of diverse leys on arable soils. J. Soil Sci. 9, 252–266.

Dinno, A., 2017. Dunn's Test of Multiple Comparisons Using Ranked Sums. RStudio, Inc., Boston, MA.

Dunn, O.J., 1964. Multiple comparisons using rank sums. Technometrics 6, 241–252.

Edwards, A.P., Bremner, J.M., 1967. Microaggregates in soils. J. Soil Sci. 18, 64–73.

Field, D.J., Minasny, B., 1999. A description of aggregation liberation and dispersion in A horizons of Australian Vertisols by ultrasonic agitation. Geoderma 91, 11–26.

Field, D.J., Minasny, B., Gaggin, M., 2006. Modelling aggregation liberation and dispersion of three soil types exposed to ultrasonic agitation. Aust. J. Soil Res. 44, 497–502.

Fristensky, A., Grismer, M.E., 2008. A simultaneous model for ultrasonic aggregate stability assessment. Catena 74, 153–164.

Gee, G.W., Bauder, J.W., 1986. Particle-size analysis. In: Klute, A. (Ed.), Methods of Soil Analysis. Part 1, 2nd ed. Agronomy Monographs 9 ASA and SSSA, Madison, WIpp. 383–411.

Green, R.S., Hairsine, P.B., 2004. Elementary processes of soil-water interaction and thresholds in soil surface dynamics: a review. Earth Surf. Process. Landf. 29, 1077–1091.

Harris, D., Horwáth, W.R., van Kessel, C., 2001. Acid fumigation of soils to remove carbonates prior to total organic carbon or carbon-13 isotopic analysis. Soil Sci. Soc. Am. J. 65, 1853–1856.

Hole, F.D., 1981. Effects of animals on soil. Geoderma 25, 75–112.

Hunter, C.R., Busacca, A.J., 1989. Dispersion of three andic soils by ultrasonic vibration. Soil Sci. Soc. Am. J. 53, 1299–1302.

Jacobson, B.L., Grimm, E.C., 1986. A numerical analysis of Holocene forest and prairie vegetation in central Minnesota. Ecology 67, 958–966.

Jastrow, J.D., Bouton, T.W., Miller, R.M., 1996. Carbon dynamics of aggregate-associated organic matter estimated by carbon-13 natural abundance. Soil Sci. Soc. Am. J. 60, 801–807.

Johnson, D.L., Watson-Stegner, D., Johnson, D.N., Schaetzl, R.J., 1987. Proisotropic and proanisotropic processes and pedoturbation. Soil Sci. 143, 278–292.

Jozefaciuk, G., Czachor, H., 2014. Impact of organic matter, iron oxides, alumina, silica and drying on mechanical and water stability of artificial soil aggregates. Assessment of new method to study water stability. Geoderma 221–222, 1–10.

Kasmerchak, C., 2016. Texture-Contrast Profile Development Across the Prairie-Forest Ecotone in Northern Minnesota – Physicochemical Properties That Influence Aggregation, Clay Dispersion, and Translocation. M.S. Thesis. University of Wisconsin, Madison.

Kemper, W.D., Rosenau, R.C., 1986. Aggregate stability and size distribution. In: Methods of Soil Analysis, Part 1. American Society of Agronomy – Soil Science Society of America, Madison, Wisconsin, pp. 424–442.

Lawrence, G.B., David, M.B., Shortle, W.C., 1995. A new mechanism for calcium loss in forest-floor soils. Nature 378, 162–165.

Le Bissonnais, Y., 1996. Aggregate stability and assessment of soil crustability and erodibilty. 1. Theory and methodology. Eur. J. Soil Sci. 47, 425–437.

Legout, C., Leguédois, S., Le Bissonais, Y., 2005. Aggregate breakdown dynamics under rainfall compared with aggregate stability measurements. Eur. J. Soil Sci. 56, 225–237.

Leguédois, S., Le Bissonais, Y., 2004. Size fractions resulting from an aggregate stability test, interrill detachment and transport. Earth Surf. Process. Landf. 29, 1117–1129.

Levy, G.J., Agassi, M., Smith, H.J.C., Stern, R., 1993. Microaggregate stability of kaolinitic and illitic soils determined by ultrasonic energy. Soil Sci. Soc. Am. J. 57, 803–808.

Mason, J.A., Greene, R.S.B., Joeckel, R., 2011. Laser diffraction analysis of the disintegration of aeolian sedimentary aggregates in water. Catena 87, 107–118.

Mason, J.A., Jacobs, P.M., Greene, R.S.B., Nettleton, W.D., 2003. Sedimentary aggregates in the Peoria Loess of Nebraska, USA. Catena 53, 377–397.

McAndrews, J., 1966. Postglacial history of prairie, savannah, and forest in northwestern Minnesota. Torrey Botanical Club Memoir 22, 1–72.

McAndrews, J., 1967. Pollen analysis and vegetational history of the Itasca region, Minnesota. In: Cushing, E., Wright Jr.H.E. (Eds.), Quaternary Paleoecology. Yale University Press, New Haven, pp. 219–239.

Mikutta, R., Mikutta, C., Kalbitz, K., Scheel, T., Kaiser, K., Jahn, R., 2007. Biodegradation of forest floor organic matter bound to minerals via different binding mechanisms. Geochim. Cosmochim. Acta 71, 2569–2590.

Muggler, C.C., Pape, T.H., Buurman, P., 1997. Laser grain size determination in soil genetic studies: 2. Clay content, clay formation, and aggregation in some Brazilian Oxisols. Soil Sci. 162, 219–228.

Neilsen, G.A., Hole, F.D., 1964. Earthworms and the development of coprogeneous A1 horizons in forest soils in Wisconsin. Soil Science Society of America 54, 426–430.

Nelson, D., Hu, F., 2008. Patterns and drivers of Holocene vegetational change near the prairie-forest ecotone in Minnesota: revisiting McAndrews' transect. New Phytol. 179, 449–459.

Nimmo, J.R., Perkins, K.S., 2002. Aggregate stability and size distribution. In: Dane, J.H., Topp, G.C. (Eds.), Methods of soil analysis, Part 4—Physical Methods. Soil Science Society of America, Madison, WI, pp. 317–328.

North, P.F., 1976. Towards an absolute measurement of soil structural stability using ultrasound. J. Soil Sci. 27, 451–459.

Oades, J.M., 1984. Soil organic matter and structural stability: mechanisms and implications for management. Plant Soil 76, 319–337.

Oades, J.M., 1988. The retention of organic matter in soils. Biogeochemistry 5, 35–70.

Oades, J.M., 1993. The role of biology in the formation, stabilization and degradation of soil structure. Geoderma 56, 377–400.

Parton, W.J., Schimel, D.S., Cole, C.V., Ojima, D.S., 1987. Analysis of factors controlling soil organic matter levels in Great Plains grasslands. Soil Sci. Soc. Am. J. 51, 1173–1179.

Pennock, D., Bedard-Haughn, A., Viaud, V., 2011. Chernozemic soils of Canada: genesis, distribution, and classification. Can. J. Soil Sci. 91, 719–747.

Raine, S.R., So, H.B., 1993. An energy-based parameter for the assessment of aggregate bond-energy. J. Soil Sci. 44, 249–259.

Ramnarine, R., Voroney, R.P., Wagner-Riddle, C., Dunfield, K.E., 2011. Carbonate removal by acid fumigation for measuring the $\delta^{13}C$ of soil organic carbon. Can. J. Soil Sci. 91, 247–250.

Rawlins, B.G., Turner, G., Wragg, J., McLachlan, P., Lark, R.M., 2015. An improved method for measurement of soil aggregate stability using laser granulometry applied at regional scale. European Journal of Soil Research 66, 604–614.

Rawlins, B.G., Wragg, J., Lark, R.M., 2013. Application of a novel method for soil aggregate stability measurement by laser granulometry with sonication. European Journal of Soil Research 64, 92–103.

RStudio Team, 2015. RStudio: Integrated Development for R. RStudio, Inc., Boston, MA.

Schaetzl, R.J., 1986. Complete soil profile inversion by tree uprooting. Phys. Geogr. 7, 181–189.

Schaetzl, R.J., Thompson, M.L., 2015. Soils Genesis and Geomorphology, 2nd ed. Cambridge University Press, New York.

Severson, R., Arneman, H., 1973. Soil characteristics of the forest-prairie ecotone in northwestern Minnesota. Soil Sci. Soc. Am. Proc. 37, 593–599.

Singer, M.J., Shainberg, I., 2004. Mineral soil surface crusts and wind and water erosion. Earth Surf. Process. Landf. 29, 1065–1075.

Six, J., Bossuyt, H., Degryze, S., Denef, K., 2004. A history of research on the link between (micro)aggregates, soil biota, and soil organic matter dynamics. Soil Tillage Res. 79, 7–31.

Six, J., Elliot, E.T., Paustian, K., Doran, J.W., 1998. Aggregation and soil organic matter accumulation in cultivated and native grassland soils. Soil Sci. Soc. Am. J. 62, 1367–1377.

Thomas, G.W., 1982. Exchangeable cations. In: Page, A.L., Miller, R.H., Keeney, D.R. (Eds.), Methods of Soil Analysis. Part 2 Chemical and Microbiological Properties, 2nd ed. American Society of Agronomy, Madison, Wisconsin, pp. 159–165.

Tisdall, J.M., 1996. Formation of soil aggregates and accumulation of soil organic matter. In: Carter, M.R., Stewart, B.D. (Eds.), Structure and Organic Matter Storage in Agricultural Soils. CRC Press, Boca Raton, FL, pp. 57–96.

Tisdall, J.M., Oades, J.M., 1982. Organic matter and water-stable aggregates in soils. J. Soil Sci. 62, 141–163.

von Lutzow, M., Kogel-Knabner, I., Ekschmitt, K., Fless, H., Guggenberger, G., Matzner, E., Marschner, B., 2007. SOM fractionation methods; relevance to functional pools and to stabilization mechanisms. Soil Biol. Biochem. 39, 2183–2207.

von Lutzow, M., Kogel-Knabner, I., Ludwig, B., Matzner, E., Fless, H., Ekschmitt, K., Guggenberger, G., Marschner, B., Kalbitz, K., 2008. Stabilization mechanisms of

organic matter in four temperate soils: development and application of a conceptual model. J. Plant Nutr. Soil Sci. 171, 111–124.
Webb III, T., Cushing, E., Wright Jr., H.E., 1983. Holocene changes in vegetation of the Midwest. In: Wright Jr.H.E. (Ed.), Late-Quaternary Environments of the United States, Vol. 2. The Holocene. University of Minnesota Press, Minneapolis, MN, pp. 142–165.
Westerhof, R., Buurman, P., van Griethuysen, C., Ayarza, M., Vilela, L., Zech, W., 1999. Aggregation studied by laser diffractionn relation to plowing and liming in the Cerrado region in Brazil. Geoderma 90, 277–290.
Whitlock, C., Bartlein, P.J., Watts, W.A., 1993. Vegetation history of Elk Lake. In: Bradbury, J.P., Dean Walter, E. (Eds.), Elk Lake, Minnesota; Evidence for Rapid Climate Change in the North-Central United States. Geological Society of America (GSA), Boulder, CO, United States, pp. 251–274.
Wright Jr., H.E., 1976. The dynamic nature of Holocene vegetation: a problem in paleoclimatology, biogeography, and stratigraphic nomenclature. Quat. Res. 6, 581–596.
Yoder, R.E., 1936. A direct method of aggregate analysis of soils and a study of physical nature of erosion losses. Journal of America Society of Agronomy 28, 337–351.